Vol 14 No 3, March 2005
1009-1963/2005/14(03)/0634-08

Chinese Physics

© 2005 Chin. Phys. Soc.
and IOP Publishing Ltd

Overtone spectrum of SiH stretching in H_2SiCl_2*

Chen Ping(陈 平)[a], Zhu Huai(朱 淮)[b]†, Hao Lu-Yuan(郝绿原)[a]‡,
Hu Sui-Ming(胡水明)[a], Liu An-Wen(刘安雯)[a],
Zheng Jing-Jing(郑晶晶)[a], and Ding Yun(丁 昀)[a]

[a] *Bond Selective Chemistry, University of Science and Technology of China, Hefei* 230026, *China*

[b] *Department of Basic Education for Information, Anhui College of Traditional Chinese Medicine, Hefei* 230038, *China*

(Received 4 September 2003; revised manuscript received 2 November 2004)

The overtone spectra of H_2SiCl_2 molecule in the regions of 2000–9000cm^{-1} and 12000–12900cm^{-1} at room temperatures have been studied by use of high-resolution Fourier transform spectroscopy and sensitive-intracavity-laser absorption spectroscopy, respectively. The variations of vibrational quantum numbers $\Delta V_{\rm SiH}$=1, 2, 3, 4 and 6 for the overtones of the SiH stretching have been analysed and assigned with the local mode model and the normal mode model. The values of harmonic frequency $\omega_{\rm m}$, anharmonicity constant $\chi_{\rm m}$, bond coupling constant λ, the Morse oscillator parameters $D_{\rm e}$, α, and interaction force constant $f_{rr'}$ are derived from the experimental spectrum with nonlinear least-squares fitting. The most striking feature of the SiH_2Cl_2 is that the larger the vibrational energy, the smaller the energy difference between a couple of lowest stretching states of a given manifold, and finally, the couple of lowest stretching states are degenerated within the experimental error for $\Delta V_{\rm SiH} \geq$4 vibrational manifolds. The degenerate energy level structure resembles that of a diatomic Morse oscillator; the transition energies show a remarkable fit to the Birge–Sponer relation. The high vibrational states can be described straightforward with a SiH diatomic Morse oscillator wavefunction, this is an indication of vibrational bond localization.

Keywords: local mode, normal mode, stretching vibration, molecular symmetry
PACC: 9575F; 3310

1. Introduction

Overtone spectroscopy of the polyatomic molecule is important to the fields of chemistry and physics in which are involved, for example, highly vibrationally excited molecules,[1] thermally induced chemical reactions, spectroscopy of astrophysical molecules, and multi-photon infrared photochemistry. Many investigations of overtone transitions have been concerned mainly with the molecules containing O–H or C–H bonds.[2] It is of interest to extend the overtone work to other X–H moieties:[3,4] for example, the Si–H vibrations. The fundamental vibrations of SiH_2Cl_2 in the gaseous phase have been recorded by Hawkins and Wilson,[5] and Christensen and Nielsen;[6] the vibrational assignment, description of the vibrational modes, species, and the rotational contours were given by the normal mode model. The Si–H stretching yields the values of ν_1 (A_1)=2224cm^{-1} and ν_2 (B_1)=2237cm^{-1}, where ν_1 is mainly for an symmetric SiH stretching mode, and ν_2 for an antisymmetric SiH stretching mode. The high overtones of H_2SiCl_2 for $\Delta V_{\rm SiH}$=6–9, which are in the near-IR and visible spectral regions, were recorded by Bernheim *et al* with a photoacoustic detection.[7] In this high vibrational energy region, the molecule exhibits simple progression of weak absorption features which are described as excitations of the vibrational overtones of individual Si–H stretching oscillators. The B/C hybrid of the band contours indicates the degenerate of the Si–H vibrations, which have different modes. The intermediate cases, which cover the absorption spectra of H_2SiCl_2 for $\Delta V_{\rm SiH}$=1–4 and 6, interest us because they will show the transition of the couple lowest stretching states from separation to degenerate within the given V (vibrational quantum number) vibrational manifolds as the quantum number increases, and are expected to provide insight into the possible coupling mechanisms between identical Si–H bonds. For these reasons we measured the infrared spectrum of H_2SiCl_2 in the regions of 2000–9000cm^{-1} and 12000–

*Project supported by the National Natural Science Foundation of China (Grant Nos 10274077, 20103007 and 29703007).
†Authors to whom correspondence should be addressed. E-mail: zhuhuai_hf@hotmail.com
‡E-mail: hly@ustc.edu.cn

12900cm^{-1} by use of high-resolution Fourier transform spectroscopy (FTS) and sensitive-intracavity-laser absorption spectroscopy (ICLAS), respectively. In this spectrum region, we have observed not only the expected Si–H stretching overtones but also weak absorption features which we assigned as combinations of the Si–H stretching vibration.

The H_2SiCl_2 molecule has C_{2v}-symmetry. Because the fundamental frequency of the Si–Cl bond ($\leq$530cm^{-1}) is much smaller than that of Si–H stretching, which is found at 2224cm^{-1}, there is no obvious feature of coupling between SiCl and SiH at high excitation. Thus in the case of the SiH bond, the SiH vibrations in SiH_2Cl_2 are analogous to the vibrations in XH_2 (X=O,S, and Se) systems.[8,9] The fundamental frequency of SiH_2-bending is 954cm^{-1}, which is also smaller than half of the frequency of SiH_2-stretching, hence the coupling between the SiH-stretching and the bending is negligible. Under this circumstance, the SiH stretching vibrations in H_2SiCl_2 can be investigated with two equivalent models established respectively by Child, Halone, Lehmann, and Mills and Robiette for XH_2-type molecules:[8–11] the local mode model and the normal mode model with Darling–Dennison resonance included (NMDD). Based on the two models, we have determined the location and assignment of the overtone and combination bands of the SiH stretching vibrations, and can calculate the spectral parameters and analyse the wavefunctions in relation to their local mode or normal coordinate character. The present work shows that the two models can provide a satisfactory description of the observed spectrum, and interpret why the lowest energy components of a stretching manifold are degenerate at high vibrational excitation.

2. Experimental details

Dichlorosilane gas of purity 98% was purchased from Nanjing special gas factory. The absorption spectra from 2000cm^{-1} to 9000cm^{-1}, which cover SiH stretching quantum numbers ΔV_{SiH}=1–4, were recorded by a Bruker IFS 120HR Fourier transform (FT) spectrometer equipped with a multipass cell. The maximum path length is 105m. Since the spectra cover a wide range and the absorption intensities decrease with the increment of vibrational quantum number, the FT spectra were recorded under different experimental conditions, listed in Table 1.

Table 1. Experimental conditions used to record the absorption spectrum of H_2SiCl_2.

Region/cm^{-1}	Gas pressure/Pa	Detector	Absorption length/m	Beamsplitter	Source
1500–3000	157	InSb	0.1	GaF_2	Globar
1000–5000	151	MCT	33	KBr	Globar
1800–7000	8027	InSb	15	GaF_2	Tungsten
5000–9000	8027	Ge-Diode	87	GaF_2	Tungsten

The ΔV_{SiH}=6 SiH overtone absorption, which is around 12345cm^{-1}, is rather weak; therefore it was recorded with high ICLAS in combination with FTS. The cell is filled with 20.3kPa H_2SiCl_2 sample gas, the optical absorption length is 4.5km. The vibrational band we obtained is the same as that in Ref.[7]. Figure 1 depicts the experimental configuration of the FTS–ICLAS developed in our laboratory. A detailed discussion on this experimental set-up can be found in Ref.[12]. A brief description is given here.

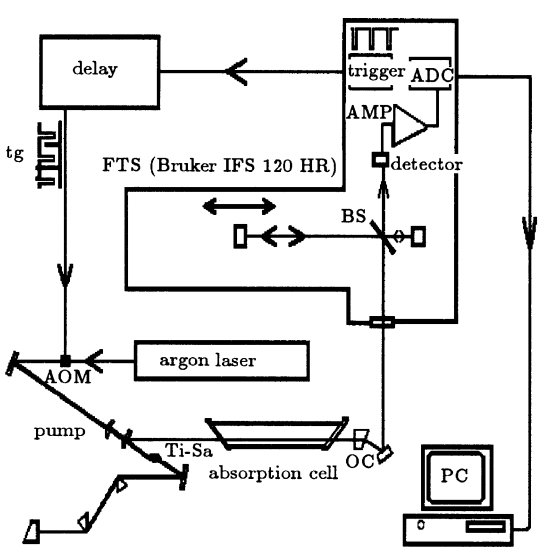


Fig.1. Configuration of the FTS–ICLAS set-up.OC: output coupler, AOM: acousto-optical modulator,Ti–Sa: Ti: sapphire crystal.

The Bruker IFS 120HR FTS with a quartz beamsplitter and a Si-diode detector is used to record the interferogram of the laser emission from a home-made 162cm long standing wave Ti:sapphire laser. The pumping laser is a coherent Verdi-5 single-mode (532nm) diode-pumped solid state laser. A 82cm long sample cell is placed inside the 151cm long Ti:sapphire laser cavity. The pumping laser beam is chopped by an acousto-optical modulator (AOM). The broad band Ti:sapphire laser emission is focused and sent into the FT interferometer. A transistor–transistor logic (TTL) signal, laser digitization (LASD) given by the FTS is used as a clock for the timing system. This signal is used to trigger a home-made function generator. The output rectangular wave from the generator, which has an adjustable delay and duration with respect to the trigger, then drives an AOM to chop the pumping laser. Thus the data acquisition of FTS and the laser emission of the ICLAS are synchronized.

The interleaved rapid-scan method implemented on the Bruker IFS 120HR FTS is used. The Blackman–Harris-3-Term is adopted as apodization function in FTS. The resolution of all the spectra is 0.2 cm^{-1}. The spectra obtained are shown in Figs.2(a), 2(b), 2(c), 2(d) and 2(e) for V_{SiH}=1, 2, 3, 4 and 6, respectively.

3. Theoretical treatment

3.1. Local mode model

The local mode model, introduced by Henry and Siebrand[13] and developed in more detail by Child and Halonen,[8] and Mills and Robiette,[11] treats a molecule containing $X-Y$ bonds as a set of loosely coupled anharmonic oscillators localized on the individual $X-Y$ bonds. The coupling arises from cross terms in both kinetic and potential energies. Using curvilinear internal coordinates and keeping the bond bending to its equilibrium configurations, the stretching Hamiltonian for XH_2 type takes the form

$$H = H^0 + H', \tag{1}$$

$$H^0 = \frac{1}{2} g_{rr}(p_a^2 + p_b^2) + D_e(y_a^2 + y_b^2), \tag{2}$$

$$H' = g_{rr'} p_a p_b + f_{rr'} r_a r_b, \tag{3}$$

where the subscripts denote individual bonds to avoid confusion with conventional normal coordinate labels; Morse variable $y = 1 - \exp(-\alpha r)$, in which α is the Morse parameter determining the harmonic force constant around equilibrium, and r is the displacement from equilibrium in the bond stretching coordinate; the momentum operator $p = -i\hbar\partial/\partial r$ (as bond a and bond b are equivalent, the subscripts a and b are omitted here); D_e is the dissociation energy from equilibrium; g_{rr} is the g matrix element given by $g_{rr} = \frac{1}{m_x} + \frac{1}{m_H} = \frac{1}{\mu}$, where $g^0_{rr'} = \cos\alpha_e / m_x$, $m_x(m_H)$ is the mass of the $X(H)$ atom, and α_e is the equilibrium SiH_2 bond angle; $f_{rr'}$ is the f matrix coupling term. H^0 is the sum of Morse bond oscillator terms, and H' is the interbond coupling term. The present formula covers a harmonic momentum and potential coupling between identical anharmonic oscillators. Expanding potential terms in H^0 gives

$$H^0 = H^0_0 + H'_0, \tag{4}$$

$$H^0_0 = \frac{1}{2} g_{rr}(p_a^2 + p_b^2) + \frac{1}{2} f_{rr}(r_a^2 + r_b^2), \tag{5}$$

and

$$H'_0 = \frac{1}{6} f_{rrr}(r_a^3 + r_b^3) + \frac{1}{24} f_{rrrr}(r_a^4 + r_b^4) + \cdots, \tag{6}$$

where f_{rr}, f_{rrr}, and f_{rrrr} are defined in a usual way as derivatives of the potential energy functions with respect to internal coordinates in the equilibrium configuration. The operator H^0_0 is the harmonic oscillator Hamiltonian for the SiH stretching vibrations. The eigenfunctions of H^0_0, in the form of product of harmonic oscillator functions of r_a and r_b, are taken as the local mode basis functions $|m,n\rangle$, corresponding to m quanta of excitation in bond a and n quanta in bond b. These singly excited bond oscillator functions $|n0\rangle$ and $|0m\rangle$ are called local mode states. Treating the H'_0 term by use of perturbation theory and eliminating the off-diagonal elements with $\Delta V \neq 0$, where $V = m + n$, an effective Hamiltonian matrix is obtained for which the diagonal matrix elements of H^0 within each V manifold are below (in wavenumber units):

$$\begin{aligned}&\langle m,n|\hat{H}/hc|m,n\rangle \\ &= \omega_m(m+n) + x_m(m^2+n^2+m+n),\end{aligned} \tag{7}$$

where the energies are measured from the zero point level $\omega_m + \frac{1}{2}\chi_m$. H' gives the matrix elements in Eqs.(8a) and (8b) (in wavenumber units):

$$\langle m+1, n-1|\hat{H}/hc|m,n\rangle = \lambda\left[(m+1)n\right]^{1/2}, \tag{8a}$$

$$\langle m-1, n+1|\hat{H}/hc|m,n\rangle = \lambda\left[m(n+1)\right]^{1/2}, \tag{8b}$$

where harmonic frequency $\omega_m = \frac{\alpha}{2\pi c}\left(\frac{2D_e}{\mu}\right)^{\frac{1}{2}}$, anharmonicity constant $x_m = \frac{\alpha^2\hbar}{4\pi c\mu}$, and bond coupling

constant $\lambda = \frac{\omega_m}{2}\left(\frac{g_{rr'}}{g_{rr}} + \frac{f_{rr'}}{f_{rr}}\right)$. This is the harmonically coupled anharmonic-oscillator model (HCAO). In this approximation, the non-zero coupling matrix elements couple states within the same ($V = m + n$) manifold. The spectroscopic parameters of this model are ω_m, χ_m and λ, as shown in Eqs.(7) and (8). The extension to couple states within different manifolds is achieved by using the products of the eigenfunctions of H^0 as basis set. This more precise Hamiltonian matrix includes all off-diagonal elements; in other words, it includes the intermanifold and intramanifold coupling, and is named the anharmonically coupled anharmonic-oscillator model (ACAO).[14−16] All the matrix elements are calculated analytically using the known formulae. The three parameters in this model are D_e, α and $f_{rr'}$; their meanings are outlined above. The eigenvalues and eigenvectors of the Hamiltonian (1) can be obtained variationally by using a harmonic oscillator basis set for the HCAO or a Morse oscillator basis set for the ACAO. By fitting the eigenvalues of Hamiltonian (1) with the experimental spectra, the parameters are deduced.

3.2. NMDD model

The NMDD model is the normal mode model with Darling–Dennison resonance included. It is developed by Lehmann[10], and Mills and Robiette[11] in a study of local mode and normal model vibrational behaviours of molecules. In this model, the Hamiltonian (Eqs.(1)–(3)) of SiH_2 stretching was transformed from curvilinear internal coordinate (r) and momenta (p_a, p_b) to normal coordinate (q) and momenta (p). This gives

$$\hat{H} = \hat{H}^0 + \hat{H}'_1 + \hat{H}'_2, \tag{9}$$

$$\hat{H}^0/hc = \frac{1}{2}\omega_m(q_1^2 + p_1^2) + \frac{1}{2}\omega_m(q_6^2 + p_6^2), \tag{10}$$

$$\hat{H}'_1/hc = \frac{1}{6}\phi_{111}(q_1^3 + 3q_1q_6^2) + \frac{1}{24}\phi_{1111}(q_1^4 + 6q_1^2q_6^2 + q_6^4), \tag{11}$$

$$\hat{H}'_2/hc = \frac{1}{2}\omega_m\left[\frac{g_{rr'}}{g_{rr}}(p_1^2 - p_6^2) + \frac{f_{rr'}}{f_{rr}}(q_1^2 - q_6^2)\right], \tag{12}$$

where the subscript figures 1 and 6 respectively denote symmetric stretching and antisymmetric stretching modes in the customary normal mode labelling scheme.

Eigenfunctions of $\hat{H}^0$ are the basis functions of harmonic oscillator normal mode. The second-order perturbation is used for treating the cubic terms in Eq.(11) and the first order for treating Eq.(12) and the quartic terms in Eq.(11) to obtain an effective Hamiltonian matrix diagonal in ΔV=0, and the matrix elements off-diagonal in $\Delta V \neq 0$ were neglected. The Darling–Dennison resonance term k_{1166} contributes off-diagonal matrix elements according to the selection rules $\Delta v_1 = \pm 2$ and $\Delta v_6 = \mp 2$. The non-zero matrix elements (taking out the zero point energy) are given by the formulae

$$\langle v_1, v_6|H|v_1, v_6\rangle = \omega_m v + \lambda(v_1 - v_6) + \frac{1}{2}x_m(v^2 + 3v + 2v_1v_6), \tag{13}$$

$$\langle v_1 + 2, v_6 - 2|H|v_1, v_6\rangle = \frac{1}{2}x_m[(v_1 + 1)(v_1 + 2)v_6(v_6 - 1)]^{1/2}, \tag{14a}$$

$$\langle v_1 - 2, v_6 + 2|H|v_1, v_6\rangle = \frac{1}{2}x_m[v_1(v_1 - 1)(v_6 + 1)(v_6 + 2)]^{1/2}, \tag{14b}$$

where

$$\omega_1 = \omega_m + \lambda, \quad \omega_6 = \omega_m - \lambda, \tag{15}$$

$$x_{11} = x_{66} = \frac{x_{16}}{4} = \frac{k_{1166}}{4} = \frac{x_m}{2}, \tag{16}$$

Here, v_1 and v_6 are vibrational quantum numbers of symmetrical stretching vibration and asymmetrical stretching vibration, respectively, and $v = v_1 + v_6$; the meaning of ω_m, x_m and λ is the same as that in local mode model respectively. Equation (13) is of diagonal elements of matrix, which is the customary expression for the anharmonic corrections to the energy levels in a polyatomic molecule with two normal modes of vibration. Equations (14a) and (14b) are of off-diagonal elements of the $\hat{H}$ matrix, which describe the Darling–Dennison resonance interaction between overtones of v_1 and v_6. That NMDD model and the HCAO model are exactly equivalent has been proved by Lehmann.[10], and Mills and Robiette.[11]

4. Results and discussion

4.1. Vibrational energy levels

Figure 2 shows gas phase infrared absorption spectra for H_2SiCl_2 in the regions of various SiH overtone absorptions.

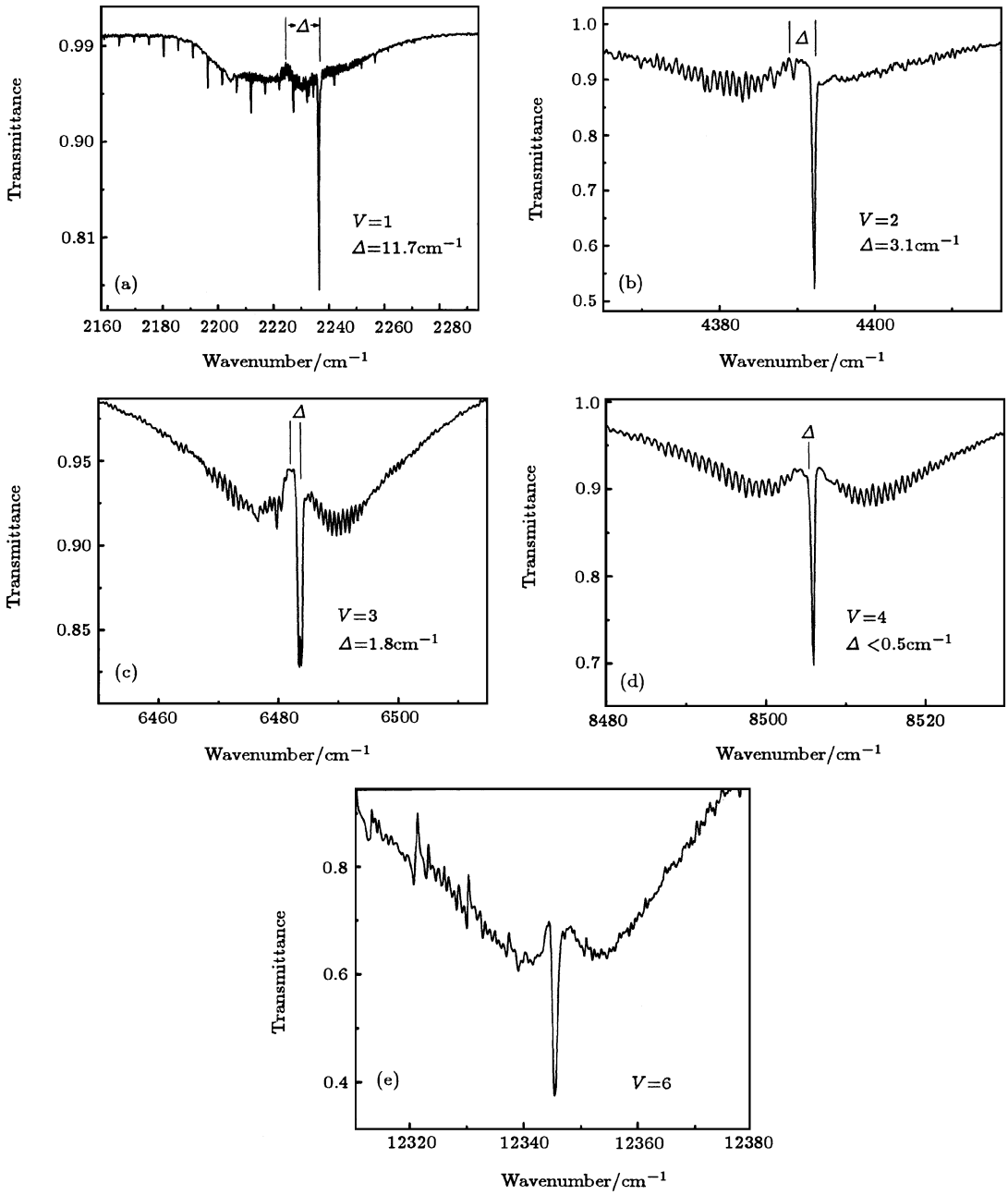


Fig.2. Vibrational spectra of H_2SiCl_2 for the couple of lowest SiH_2 stretching states. (a), (b), (c), (d) and (e) are for ΔV_{SiH}=1, 2, 3, 4 and 6 respectively. Δ is the difference between vibrational frequencies of the couple of lowest stretching states of a given manifold.

The band contour appears to be of a B/C hybrid, because the SiH stretching causes B_1-vibration and A_1-vibration, which correspond to a C-type band and a B-type band, respectively,[6] arising from transitions to states belonging to A_1 and B_1 representations of C_{2v}. From the figure we can see that the larger the vibrational energy is, the smaller the gaps between the C-type and the B-type bands is, and finally, they are degenerate within the experimental error as $\Delta V_{SiH} \geq 4$. The latter is consistent with the behaviour for ΔV_{SiH}=6–9 observed by Bernheim *et al.*[7]

The two models discussed in Section 3 are used for analysing the SiH stretching overtone. The basis set size used for both local mode and normal mode are such that $m + n \leq 6$ and $\nu_1 + \nu_6 \leq 6$, where m and n are quantum numbers for the stretching vibrations in the internal coordinate representation, ν_1 and ν_6 are quantum numbers for the stretching vibrations in the normal coordinate representation. Hamiltonian matrices of both models are diagonalized to give rise to the eigenvalues and eigenvectors. The spectroscopic

parameters, ω_m, χ_m and λ in NMDD and HCAO, D_e, α and $f_{rr'}$ in ACAO, are optimized by the nonlinear least-squares fitting using vibrational band origins as data in the fit. The observed SiH stretching vibrational band origins, the vibrational assignment with normal mode and local mode model models, and the fits, are given in Table 2. The spectroscopic parameters are presented in Table 3. Table 2 also gives a comparison between the observed and the calculated level positions by use of the NMDD, HCAO, ACAO models, and shows clearly that the present models reproduce the experimental levels well.

Table 2. Observed and calculated band centres (in cm^{-1}) of H_2SiCl_2 stretch vibration by use of NMDD, HCAO and ACAO modes.

Normal	Local	Obs.	Ref.	Obs–Cal.		
$\nu_1\nu_6$	$mn^{\pm}$			NMDD	HCAO	ACAO
1 0	10^+	2224.8[a]	2224[b]	0.1000	0.1000	–0.2000
0 1	10^-	2236.5[a]	2237[b]	0	0	–0.1000
2 0	20^+	4389.1[a]	4389[c]	–1.1000	–1.0000	–1.1000
1 1	20^-	4392.2[a]	4395[c]	0.1000	0.2000	–0.1000
0 2	11^+	4463.3[a]	4463[c]	0.1000	0.2000	–0.6000
3 0	30^+	6482.1		–14.000	–1.3000	–1.3000
2 1	30^-	6483.9[a]		0.3000	0.3000	0.3000
1 2	21^+	6610.7		–1.1000	–1.0000	–2.9000
0 3	21^-	6634.5		–0.6000	–0.5000	–1.2000
4 0	40^+	8506.0		–0.7000	–0.6000	–0.1000
3 1	40^-	8506.0[a]		–0.7000	–0.6000	–0.1000
2 2	31^+					
1 3	31^-	8715.1		–0.5000	–0.4000	–2.4000
0 4	22^+					
6 0	60^+	12345.4	12345[c]	0.2000	0.2000	2.3000
5 1	60^-	12345.4[a]	12345[c]	0.2000	0.2000	2.3000

[a] One of eight band centres is used in the fitting of the parameters in Table 3.
[b] From Ref.[6].
[c] From Ref.[7].

Table 3. Effective spectroscopic constants of H_2SiCl_2.

	NMDD	HCAO	ACAO
ω_m/cm^{-1}	2299.85(24)[a]	2299.78 (24)[a]	
x_m/cm^{-1}	–34.60(4)[a]	–34.59(8)[a]	
λ/cm^{-1}	–5.85(2)[a]	–5.87(17)[a]	
D_e/cm^{-1}	–	–	38109.67 (54.61)[a]
α/nm^{-1}	–	–	14.2(0)[a]
$f_{rr'}/cm^{-1}nm^{-2}$	–	–	111681(28.35)[a]
SD[b]$/cm^{-1}$	0.333	0.311	0.915

[a] Uncertainties are given in parentheses in the unit of last significant digit
[b] Root mean-square of the fitting residual

The two important quantities are the Morse anharmonicity parameter χ_m, which determines the diagonal energy differences, and the coupling strength λ, which determines the observed frequency splitting between vibrations associated with the identical XH bonds. According to Eqs.(7) and (8), for the $v = n$ manifold, the local mode states $|n0\rangle$ and $|0n\rangle$ are coupled with $|n-1,1\rangle$ and $|1,n-1\rangle$, respectively. The energy difference between their diagonal elements is $2(n-1)\chi_m$, while that between the off-diagonal elements is $\sqrt{n}\lambda$. Therefore, when the vibrational quantum number $v = n$ increases with the cooperation of $\chi_m \gg \lambda$, the states $|n0\rangle$ and $|0n\rangle$ become progressively decoupled from the rest of the manifolds as n in-

creases, and finally the coupling diminishes and the local mode states tend to be the eigenstates. This is why the local mode doublet splitting decreases with the increasing of energy for a molecule with non-negligible $\lambda/\chi_{\rm m}$. From the above discussion, we see that the strong vibrational anharmonicity and the high vibrational energy are key factors to the vibrational bond localization.

4.2. Coupling intensity λ

There exist the various contributions to the strength of interbond coupling λ, the momentum terms from which $g_{rr'}$ and g_{rr} may be deduced based on the knowledge of the valence-coordinate G matrix for a symmetrical XY_2 molecule with bond length r and interbond angle $\alpha_{\rm e}$: $g_{rr'}=\cos\alpha_{\rm e}/m_x$, where m_x is the effective mass of fragment $SiCl_2$,[17] and its value is 75, and $g_{rr}=1/\mu$, where μ denotes the X–H reduced mass with an approximate value of 1. The interbond angle $\alpha_{\rm e}$ in SiH_2 is 111.3^0, then the momentum coupling contribution of $\dfrac{\omega g_{rr'}}{2g_{rr}}$ to λ is –5.57, which may be compared with the full value of $-5.8{\rm cm}^{-1}$. The potential term, namely $\dfrac{\omega f_{rr'}}{2f_{rr}}$, where $f_{rr}=2a^2D_{\rm e}$, gives $-0.5{\rm cm}^{-1}$, using the derived parameter values given in Table 3. So it makes only a small amount of contribution to λ, and the potential coupling is relatively unimportant. Thus the dominant interbond coupling comes from the kinetic energy.

4.3. Vibrational wavefunction

The vibrational eigenfunctions of the two lowest energy levels of V=4 manifold obtained from the NMDD and HCAO models are compared. The NMDD gives rise to the eigenfunctions of the couple of the lowest eigenstates:

$$\varphi_{40}=0.3147|40)-0.5355|22)-0.7837|04), \quad (17)$$

$$\varphi_{31}=-0.6653|13)-0.7466|31). \quad (18)$$

Although the normal mode model is highly successful in describing the low vibrational states of most polyatomic molecules, we can see that the description of the V=4 vibration is complicated using a normal mode representation. The reason for this is that at high excitation the effect of the anharmonic terms in potential increases considerably, and then results in the coupling between the different vibrational modes; thus the traditional picture of multiple mode vibration becomes very complicated.

With the HCAO model, the couple of the lowest eigenstates for V=4 manifold are

$$\phi_{40}=0.7059(|40\rangle+|04\rangle)+0.04032(|31\rangle-|13\rangle)+0.00808|22\rangle, \quad (19)$$

$$\phi_{04}=0.7059(|40\rangle-|04\rangle)+0.04032(|31\rangle+|13\rangle)+0.00808|22\rangle. \quad (20)$$

Because the two lowest energy levels of V=4 manifold are near-degenerate, the linear combination of ϕ_{40} with ϕ_{04} is also the vibration eigenstate. Thus, by adding ϕ_{40} to ϕ_{04} or subtracting ϕ_{04} fromϕ_{40} and neglecting the terms with small coefficients, the eigenfunctions for the near-degenerate energy level take the forms of

$$\psi_{40}=\phi_{40}+\phi_{04}=|40\rangle, \quad (21)$$

$$\psi_{04}=\phi_{40}-\phi_{04}=|04\rangle. \quad (22)$$

This result shows that the singly excited bond oscillator function $|40\rangle$ or $|04\rangle$ gives a more compact description of the molecule at high vibrational excitation than does the traditional picture of multiple excitation of the normal vibrations. That is to say, the molecule can be viewed as a single-bond oscillator, and the vibrational state with a single-bond oscillation is a molecular eigenstate. The success of the local mode model stems from its ability to include the more realistic anharmonic potential function for the highly excited Si–H oscillators by using an internal coordinate system centred on the individual Si–H bonds. The bond oscillator quantum 4 or 0 is a 'good' quantum number.

The functions $|n0\rangle$ and $|0n\rangle$ are degenerate eigenfunctions of H^0. The fact that $|n0\rangle$ is a molecular eigenstate shows that the H^0 is approximately the Hamiltonian for SiH stretching motion in H_2SiCl_2, and the kinetic and potential interaction term H' can be neglected at high vibration. The term value expansion for H^0 is

$$G(m,n)=\frac{E(m,n)}{hc}=\omega_{\rm m}(m+n+1)+\chi_{\rm m}\left[\left(m+\frac{1}{2}\right)^2+\left(n+\frac{1}{2}\right)^2\right]. \quad (23)$$

Transitions from the ground state to $|n0\rangle$ state occur with energies

$$\nu=G(n,0)-G(0,0)=An+Bn^2, \quad (24)$$

where $A=\omega_{\rm m}+\chi_{\rm m}$, and $B=\chi_{\rm m}$. This is just the one-dimensional Birge–Sponer equation.[18] Equation

(26) provides a satisfactory fit for ΔV_{SiH}=4, 6–9 high overtones of H_2SiCl_2, as shown in Table 4. This fact makes it clear that as the stretching vibrations become more highly excited, the singly excited bond oscillator functions $|n0\rangle$ or $|0m\rangle$ approach closer to the eigenstates.

Table 4. Fitting result by "Birge–Sponer" relation for SiH single-bond oscillator.

Vibrational states	Obs./cm^{-1}	(Obs.–Cal.)/cm^{-1}
40	8506.0	–0.13
60	12345.4	0.46
70	14161.8	0.81
80	15913.0	–2.46
90	17588.4	1.25
ω_m/cm^{-1}	2298.5	
x_m/cm^{-1}	–34.4	
σ/cm^{-1}	1.30	

5. Conclusion

In this work the level spacing was observed to decrease with the increasing of excitation in the lowest local-mode states in H_2SiCl_2 and it is revealed that the variations in level spacing can be interpreted as an indication of incipient decoupling between symmetry related bond vibrations in certain states. The cause of this decoupling was shown to be strong bond anharmonicity which can quench interbond coupling terms arising either from potential- or kinetic-energy terms in the Hamiltonian. Analysis of the origin of the interbond coupling shows that in H_2SiCl_2 the dominant mechanism was momentum coupling. The potential coupling was relatively unimportant.

The two models are found to give a much better fit to the spectrum of H_2SiCl_2. For the energy level structure, the two models lead to identical results. However, at high vibrational excitation, the Morse oscillator wavefunctions, i.e. local mode wavefunctions, are approximately the eigenstates, and the molecule can be viewed as a single-bond oscillator.

References

[1] West G A, Barrett J J, Siebert D R and Reddy K V 1983 *Rev. Sci. Instrum.* **54** 797

[2] Zhu J and Gou Q Q 2001 *Chin. Phys.* **10** 286

[3] Chen X R, Gou Q Q and Pan X F 1998 *Acta Phys. Sin.* (Overseas Edition) **7** 327

[4] Chen X R, Chen Y, Luo J, Gou Q Q and Pan X F 1999 *Acta Phys. Sin.* (Overseas Edition) **8** 131

[5] Hawkins J A and Wilson M K 1953 *J. Chem. Phys.* **21** 360

[6] Christensen D H and Nielsen O F 1968 *J. Mol. Spectrosc.* **27** 489

[7] Bernheim R A, Lampe F W and Okeefe J F 1983 *Chem. Phys. Lett.* **100** 45

[8] Child M S and Halonen L 1984 *Adv. Chem. Phys.* **57** 1

[9] Halone L 1988 *J. Chem. Phys.* **88** 7599

[10] Lehmann K K 1983 *J. Chem. Phys.* **79** 1098

[11] Mills I M and Robiette A G 1985 *Mol. Phys.* **56** 743

[12] Cheng J X, Lin H, Hu S M, He S G and Zhu Q S 2000 *Appl. Opt.* **39** 2221

[13] Henry B R and Siebrand W 1968 *J. Chem. Phys.* **49** 5369

[14] Child M S and Halonen L 1984 *Adv. Chem. Phys.* **57** 1

[15] Halonen L and Child M S 1982 *Mol. Phys.* **46** 239

[16] Halonen L and Child M S 1988 *Comput. Phys. Commun.* **51** 173

[17] Chen P, Zheng J J, Liu A W, He S G, Hu S M and Hao L Y 2003 *Chin. J. Chem. Phys.* **16** 167

[18] Birge R T and Sponer H 1926 *Phys. Rev.* **28** 259